Overlayer growth and electronic properties of the Bi/GaSb(110) interface

Luca Gavioli, Maria Grazia Betti, Paolo Casarini, and Carlo Mariani
Dipartimento di Fisica, Università di Modena, via G. Campi 213/A, I-41100 Modena, Italy
(Received 27 December 1994)

The overlayer growth and electronic properties of the Bi/GaSb(110) interface and of the two-dimensional ordered (1×1)- and (1×2)-Bi layers have been investigated by complementary spectroscopic techniques (high-resolution electron-energy-loss, photoemission, and Auger spectroscopy). Bismuth forms an epitaxial monolayer, followed by island formation (Stranski-Krastanov growth mode) covering an average surface area of 40% at a nominal coverage of 4 ML. The (1×2)-symmetry stable structural phase, obtained after annealing at ~220 °C, corresponds to an average nominal Bi coverage of about 0.7 ML, suggesting an atomic geometry different from the epitaxial-continued layer structure. The disposal of Bi atoms in the (1×2) structure should build up an "open" layer, as the Ga-related surface exciton quenched in the (1×1) epitaxial monolayer is present in the (1×2) stable phase. The two symmetry phases are characterized by strong absorption features at 1 eV [(1×1)-Bi] and 0.54 eV [(1×2)-Bi], related to interband electronic transitions between Bi-induced electronic states. The major Bi-related occupied electronic levels, present in the valence band of the (1×1)- and (1×2)-Bi layer, have been detected by angle-integrated ultraviolet photoemission spectroscopy. Both the (1×1) and (1×2) phases show a metallic nature, with a low density of electronic states at the Fermi level. Schottky barrier heights of 0.20 and 0.14 eV are estimated for the epitaxial (1×1)- and (1×2)-symmetry stage, respectively, by analyzing the space-charge layer conditions through the study of the dopant-induced free-carrier plasmon in the GaSb substrate.

I. INTRODUCTION

The deposition of group-V semimetals (Sb, Bi) at room temperature (RT) on the (110) surface of III-V compound semiconductors has been a topic of much interest in the last few years. In fact, they build up unreactive, abrupt, and epitaxially ordered interfaces, constituting favorable two-dimensional (2D) ordered systems for studying the interrelationship between geometric structure and electronic properties.[1–19]

The epitaxial-continued layer structure (ECLS) has been the geometrical model generally employed to explain the formation of semimetal/III-V(110) interfaces. As an example, antimony forms a layer structure (ECLS) on GaAs(110),[2,3,9,14,20–23] with the Sb atoms continuing the underlying bulk structure of GaAs, and with a corresponding semiconducting character.[10,24,25] Bismuth grows with a shifted-ECLS geometry on GaAs(110),[18,26] forming dislocations, as observed by scanning tunneling microscopy,[5] and the interface remains semiconducting.[6,12]

If one considers the lattice spacing of the Sb or Bi adatoms on a given III-V(110) surface, and their peculiar bulk lattice parameter, a different value of geometric surface atomic matching can be found. In particular, a better matching is present for Sb than for Bi on GaAs(110), and this could lead one to believe that the surface atomic matching is the leading parameter for the establishment of these ordered ECLS geometries. However, a recent low-energy electron-diffraction (LEED) investigation[9] established that the stable configuration for the Bi/GaSb(110) and Bi/InSb(110) interfaces presents a (1×2)-symmetry reconstruction: thus, since the surface atomic matching in these interfaces is rather good, the lattice mismatch cannot be invoked as the only parameter producing the (1×2)-symmetry structure. It has been recently observed[27] that the chemical interaction between the adatoms and the substrate influences the hybridization of the covalent overlayer-substrate bonds, becoming a significative issue in the establishment of surface geometry.

A valuable example underlying the importance of chemical bonding is the Bi/GaSb(110) interface, which presents the (1×2) reconstruction while having good lattice matching. The LEED data by Ford *et al.*[9] have shown that the stable (1×2) geometry, obtained through a mild annealing at ~200° of the RT-grown Bi layer, takes place along the [001] direction, perpendicular to the overlayer chains. The interrelationship between growth morphology and electronic properties of this interface is still lacking; also, the growth mode of Bi/GaSb(110) beyond the first monolayer is unknown. Angular-resolved photoemission work by McIlroy *et al.*[28] determined the Bi-induced occupied electronic levels, and a semiconducting character of this interface in contrast with our present measurements. Recent high-resolution electron-energy-loss-spectroscopy (HREELS) measurements in the energy-gap region observe a strong interband electronic transition between Bi-derived levels and the appearance of a semimetallic character at the monolayer coverage scale,[17] contrasting the behavior of other semimetal/III-V(110) interfaces.

In the present work, we approach the investigation of this interface system in its ordered 2D structures—the room-temperature-grown (1×1) and the thermally stabilized (1×2) configuration—by using complementary

spectroscopic techniques. In particular, we study the overlayer growth and morphology below and above the monolayer coverage stage, by Auger electron spectroscopy (AES). We obtain information on the growth mode of Bi, on the metallization process, and on the Bi-induced electronic states at the interface, by electron-energy-loss spectroscopies (EELS and HREELS) angle-integrated ultraviolet photoemission spectroscopy (UPS).

The paper is organized as follows. After an experimental section (II), the results and discussion (III) will be collected in five sections: the first dealing with the morphology and growth mode, by Auger electron spectroscopy (III A); the second devoted to the study of the low-energy electronic properties of the interface, by HREELS (III B); the third reporting an investigation of the occupied energy levels, by photoemission (III C); the fourth analyzing the electronic structure at high energy ($\sim$2–35 eV) and the evolution of the cation surface exciton, by EELS (III D); and the fifth dealing with the space-charge layer and metallization process, as studied by HREELS (III E). The summary and conclusions will be outlined in the last section (IV).

II. EXPERIMENT

Experiments were carried out at the surface physics laboratory Spettroscopia Elettronica Superfici Adsorbati Modena (SESAMO), at the Dipartimento di Fisica, Università di Modena. All the spectroscopic tools are contained in an ultrahigh-vacuum (UHV) apparatus containing also a LEED, which is connected through an UHV valve to a preparation chamber equipped with ancillary facilities (cleaver, evaporators, thickness monitor, etc.) for sample preparation and characterization. Base pressure in both chambers was in the 10^{-11} mbar (10^{-9} Pa) range, ensuring excellent conditions for clean interface preparation and investigation.

The HREELS measurements were taken with a Leybold-Heraeus ELS-22 spectrometer, in the specular direction, with primary beam energies (E_p) ranging between 5 and 20 eV, and with incident and collecting angles (with respect to the normal to the surface) between 63° and 65°. The energy resolution, defined as the full width at half maximum of the elastically scattered peak, was set depending on the type of experiment. It was better than 10 meV, ensuring a precision better than 1 meV in the plasmon- and phonon-energy-shift measurements, when investigating the very low-energy region (0–100 meV); it was worsened to $\sim$20 meV (a compromise to have a reasonable counting rate) when studying the low-energy electronic properties in the gap region.

A double-pass cylindrical mirror analyzer (CMA) with a coaxial electron gun was used for analysis of the kinetic energy of the electrons, in the other spectroscopic techniques. The CMA was used in the "retarding mode" at constant energy resolution (0.1 eV) for the angle-integrated UPS measurements, performed with a discharge lamp as source for the He I 21.2-eV photons. During the Auger and EELS measurements, the CMA was operated in the first derivative mode, with a voltage modulation of 2 and 0.5 V, respectively. Impinging electron currents of less than 1 μA, and primary beam energies E_p of 3000 eV (Auger) and about 100 eV (EELS) were used.

The GaSb single crystals were of different doping: moderately p-type (1.2×10^{17} cm^{-3}) and n-type ($\sim2\times10^{18}$ cm^{-3}), the latter used for the HREELS measurements in the Fuchs-Kliewer phonon and dopant-induced free-carrier plasmon-energy region (0–100 meV). The GaSb(110) surfaces were prepared by cleavage in UHV with the single-wedge technique. Bismuth was evaporated by a resistively heated quartz crucible, deposited on the substrate at RT, with the evaporation rate of about 1 Å per min. During evaporation, the pressure rose in the low 10^{-10}-mbar (10^{-8} Pa) range. The overlayer thickness was determined with an oscillating quartz microbalance and checked with Auger spectroscopy. One monolayer (ML) is defined as a Bi atomic density equivalent to the surface atomic density of GaSb(110) (7.55×10^{14} at cm^{-2}).

III. RESULTS AND DISCUSSION

A. Overlayer growth and morphology

The overlayer growth and morphology of Bi on GaSb(110) have been studied by AES. We measured low- and high-energy Ga, Sb, and Bi Auger lines, for a full characterization of the overlayer growth and morphology.[29] In the following, we pay attention to the low-energy peaks, more surface sensitive and susceptible to be influenced by any modification of the chemical environment. The evolution of the Ga-$M_{2,3}M_{4,5}M_{4,5}$, Sb-$M_{4,5}N_{4,5}N_{4,5}$, and Bi-$N_{6,7}O_{4,5}O_{4,5}$ Auger lines, taken in the first derivative mode as a function of the Bi coverage and of the annealing temperature, is shown in Fig. 1. All the Auger lines do not shift in energy, and do not show line-shape modifications in the whole coverage range and as a function of annealing temperature; the Auger peaks corresponding to the (1×2)-phase reconstruction

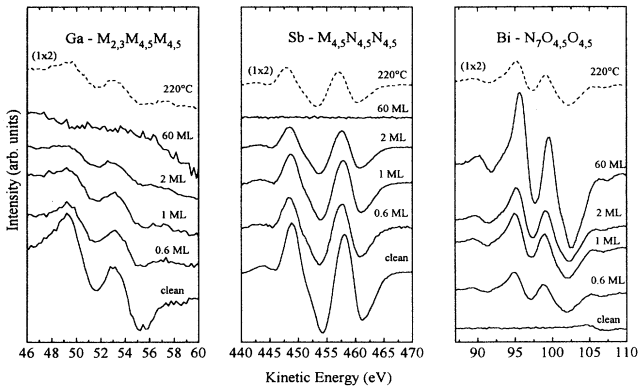

FIG. 1. Auger Ga-$M_{2,3}M_{4,5}M_{4,5}$, Sb-$M_{4,5}N_{4,5}N_{4,5}$, and Bi-$N_7O_{4,5}O_{4,5}$ peaks as a function of Bi coverage on the clean GaSb(110) surface (continuous lines), and for the (1×2)-Bi reconstructed phase after annealing (dashed line).

(~220 °C) also have the same energy and line shape observed as a function of coverage. These aspects clearly ensure the absence of surface reactivity and disruption of the interface, even if GaSb has a small heat of formation within the III-V's (~10 kcal/mol), and can undergo surface disruption upon deposition of noble[30–32] or alkali[33] metals. This lack of strong chemical interaction is a feature common to several semimetal/III-V(110) interfaces.[1,12–14,34]

The peak-to-peak intensity of the low-energy Ga and Bi Auger lines is shown in Fig. 2, as a function of the Bi coverage. A linear increase (attenuation) is detected for the Bi (Ga) peak, up to a nominal thickness of 2.7 Å, corresponding to 1-ML coverage. The first monolayer is ordered and epitaxial, as shown by the (1×1)-symmetry LEED spots. A further increase (decrease) of the Auger peaks, but with lower and varying slope, is detected at higher Bi thickness. This regular uniform growth for the first monolayer, followed by a clustering of the Bi atoms at higher coverage is a typical Stranski Krastanov (SK) growth mode.[35] A similar conclusion is drawn by van Gemmeren and Johnson[36] by studying the intensity behavior of core-level photoemission peaks for the same interface as a function of Bi coverage. Analysis of the Bi-to-Sb and Bi-to-Ga intensity ratios by means of a suitable model[37] confirms the SK growth and gives an indication of the percentage cluster-covered area above the first monolayer, i.e., ~40% on the average in the nominal coverage range ~2–4 ML,[29] increasing towards 100% at higher coverage. Thus, a relatively large average area at the surface (~60%) is free from Bi clusters, leaving patches of substrate covered by a single monolayer for a nominal average Bi thickness of more than 10 Å.

Thermal annealing of a few ML-thick RT-deposited Bi layer leads to the desorption of Bi up to the appearance of a distinct (1×2)-symmetry LEED pattern. This reconstructed phase is stable in a rather wide temperature range (~200–280 °C), so that it can be considered as the stable two-dimensional ordered structure for this interface. The evolution of the Bi-$N_7O_{4,5}O_{4,5}$ peak intensity (starting from a several ML-thick Bi layer), as a function of the annealing temperature, is shown in Fig. 3.

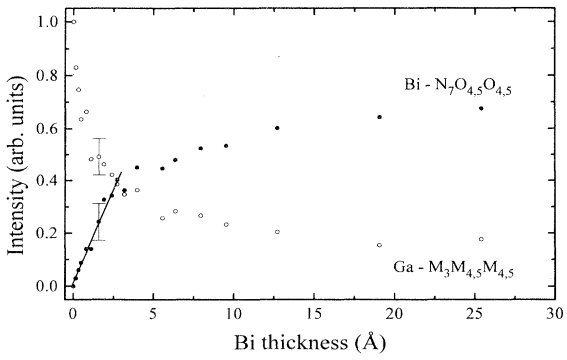

FIG. 2. Dependence of the normalized intensities of the Bi (black dots) and Ga (white dots) Auger peaks as a function of the Bi coverage on the GaSb(110) substrate.

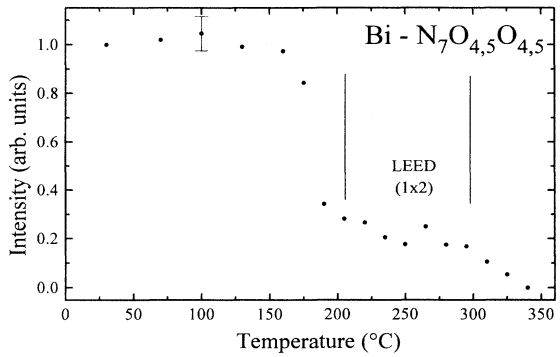

FIG. 3. Dependence of the normalized intensity of the Bi Auger peak as a function of annealing temperature, from a thick Bi layer grown on GaSb(110).

The Bi Auger peak intensity, stable up to ~175 °C attenuates and reaches a *plateau* in the ~200–280 °C temperature range. Further annealing leads to a strong attenuation of the Bi-related signal, indicating sudden desorption. The (1×2)-symmetry LEED pattern is maintained in the same temperature range where the Bi Auger signal is constant. The (1×2)-Bi phase is stable and corresponds to a constant thickness in the temperature range 200–280 °C. The estimation of the Bi coverage gives a value lower than 1 full ML (0.70±0.15 ML), in good agreement with a very recent determination by core-level photoemission analysis,[36] and close to that indicated in other photoemission work.[28] The estimated coverage value can support a structural model with an "open" two-dimensional structure corresponding to a doubling of the unit cell in the [001] direction. A geometry in which every but one row of the zig-zag chains along the [1–10] direction is removed could account for the doubled unit cell and a 0.75-ML coverage, and retain a structure resembling the ECLS. However, we cannot exclude a zigzag chain structure different from the ECLS: In fact, in very recent preliminary grazing-incidence x-ray diffraction experiments on the (1×2)-Bi/GaSb(110) interface and on the similar (1×2)-Bi/InAs(110) system, different disposal of the Bi atoms are compatible with the experimental diffraction data.[38] We shall also see how this coverage lower than 1 ML, corresponding to the (1×2)-Bi phase, is very consistent with the reappearance of the Ga-related surface exciton observed by EELS (see Sec. II D); in fact, an "open" structure at the surface can be consistent with a preferential bonding of Bi with Sb, leaving a certain fraction of free Ga dangling bonds at the origin of the excitonic interaction.

B. Low-energy electronic properties by HREELS

Electron-energy-loss structures in the semiconductor bulk-gap energy region can be related to electronic transitions involving occupied and empty surface (or adatom-induced) states. HREELS, in suitable scattering conditions, enhances surface sensitivity. The HREELS data in

the energy region of the semiconductor bulk gap for the clean GaSb(110) surface and at different Bi coverages, are collected in Fig. 4. The energy position of the loss peaks has been derived by a numerical second derivative of the data, and reported in Table I. From the data relative to the clean surface, we estimate an absorption edge of about 0.75 eV at GaSb(110), consistent with the bulk-gap value.[39] We can rule out the presence of any detectable surface states in the bulk energy gap. The loss structures at 1.20 eV (observed for the first time by HREELS (Ref. 17) and 1.45 eV (present also in previous EELS measurements by van Laar, Huijser, and van Rooy[40]) can be attributed to transitions between surface states. The structures at 1.85, ~2.1, and ~2.9 eV [previously observed by polarization-modulated reflectivity, the latter at 3 eV (Ref. 41)] can be attributed to electronic transitions from the occupied to the empty dangling-bond states localized at the surface.

The deposition of Bi causes a gap narrowing, accompanied by the growth of a main absorption band roughly centered at 1 eV in the whole coverage range up to 1 ML. The loss features relative to the clean GaSb(110) surface are quenched in the first coverage stage, rapidly overwhelmed by the growing intensity of the Bi-induced peak at 1.0 eV, with a shoulder at 1.1 eV. Another important characteristic of the (1×1)-Bi ML is the feeble continuum of intraband transitions taking place in the semiconductor band-gap region. This distinct low-energy tail (or quasielastic peak broadening) superimposed on the 1-eV Bi-induced absorption band in the HREELS data, can be ascribed to a semimetallization of the interface.[17,42] As to the very nature of the semimetallization process, a quasielastic peak broadening can be caused either by the overlap of valence and conduction bands, or even by the thermal excitation of surface free carriers across a very narrow energy gap (of the order of $k_B T$ at RT), and by electron-phonon coupling effects.[43] Thus, although a definite semimetallic character is present at the (1×1)-Bi/GaSb(110) interface, conclusive statements about the very nature of metallicity cannot be drawn. However, data taken at low temperature on the (1×2) phase do not show significant modifications in the low-energy absorption tail, favoring an interpretation based on actual semimetallic character of the stable (1×2) structure. We can reasonably infer and suggest that the low-energy absorption signal measured for the (1×1)-Bi phase is due to a partial overlap of Bi-induced electronic states with the Fermi level. Eventually, a structureless free-electron-like intraband absorption is present at a coverage of a few monolayers.

TABLE I. Energy positions (in eV) of the loss structures for the Bi/GaSb(110) interface, as deduced by a numerical second derivative of the HREELS data.

Clean GaSb(110)			1.20	1.45	1.85	~2.1	2.9
0.3-ML Bi		1.0	1.15				
0.6-ML Bi		1.0	1.1				
1-ML (1×1)-Bi		1.0	1.1				
annealed (1×2)-Bi	0.54	0.7	1.1			~2.1	

The HREELS data corresponding to the (1×2)-Bi/GaSb(110) interface is shown in Fig. 5, along with the previously discussed (1×1)-Bi phase. A huge absorption peak is observed at 0.54 eV, superimposed to a continu-

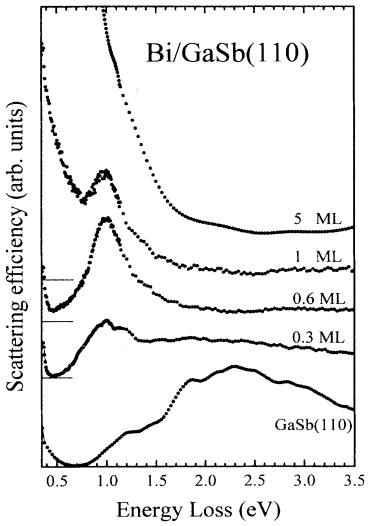

FIG. 4. HREELS (scattering efficiency) data of the Bi/GaSb(110) interface, as a function of Bi coverage, in the energy region of the fundamental bulk gap of GaSb. Spectra are normalized to their respective elastic peak heights and displaced along the vertical axis for convenience.

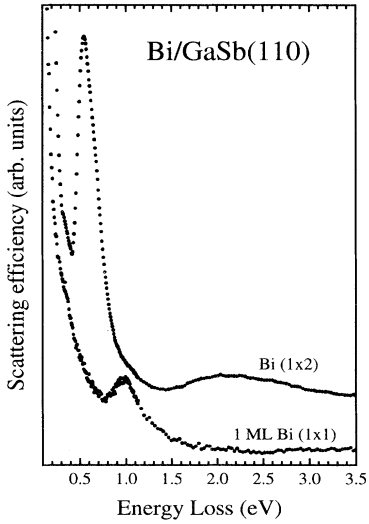

FIG. 5. HREELS (scattering efficiency) data of the (1×2)-Bi stable phase, obtained by thermal annealing, compared to the (1×1)-Bi monolayer as deposited on GaSb(110). Spectra are normalized to their respective elastic peak heights.

um of intraband transitions from the very low energies. HREELS absorption data taken at 150 K did not reveal any significant narrowing of the low-energy elastic peak tail, as would be expected from thermal promotion of free carriers to the conduction band. Thus, we can reasonably assume that the semimetallic character of the (1×2)-Bi/GaSb(110) interface is due to an actual crossing of Bi-induced electronic states with the Fermi level at certain points of the surface Brillouin zone (SBZ). The very intense 0.54-eV structure is caused by an interband electronic transition between Bi-derived occupied and empty states in the stable (1×2) geometry. It is evident that the structural reconstruction determines the electronic properties of the interface, producing a clear energy lowering of the main absorption band on passing from the (1×1) to the stable (1×2) phase.

Other features present in the HREELS data of the (1×2)-Bi phase are a broad band at ~2.1 eV and feeble shoulders at ~0.7 and ~1.1 eV (see Table I). The 2.1-eV structure is due to an interband electronic transition between Bi-induced levels; however, we can assume that the initial occupied state is different from that contributing to the main absorption peak (we shall comment later on this point, in discussing the photoemission measurements).

Azimuthal-dependent HREELS data, taken along the main symmetry directions [(1-10) or Φ=0°, and (001) or Φ=90°] are shown in Fig. 6. The main absorption structure at 0.54 eV does not show a strong anisotropy, while the 0.7-eV shoulder and the 1.1-eV peak present an azimuthal dependence: in particular, the excitation process is favored when the surface transferred momentum is oriented along the direction normal to the Bi atomic chains. However, the actual experimental conditions cannot allow a full azimuthal resolution,[44] as a consequence of the finite angular acceptance of the analyzer. Thus, the low signal at 0.7 and 1.1 eV for Φ=0° can even be due to the remnant of the structures polarized along Φ=90°.

C. Occupied electronic states by photoemission

The photoemission energy distribution curves (EDC's) in the valence-band region are shown in Fig. 7, as a function of the Bi coverage. The EDC relative to the clean GaSb(110) surface presents the main features roughly positioned at 2, 4, and 7 eV, and is consistent with previously published data.[45] Our angular-integrated measurements cannot be fully compared with previous angular-resolved photoemission data of the clean surface showing an intrinsic integrap surface state at about 0.15–0.2 eV above the valence-band maximum,[46,47] owing to the different angular acceptance of the electron analyzers. However, we do not have direct evidence of intrinsic intergap surface states. Moreover, by comparing the photoemission data with the previously shown HREELS measurements of the clean surface (Sec. III B), we notice that the lowest-energy absorption signal is measured at 0.75 eV, corresponding to the edge of the valence- to conduction-band transition; this is further evidence of lack of intrinsic gap states.

The deposition of bismuth causes a decreasing intensity of the clean surface structure, while new features emerge in the EDC's. They become particularly well defined at the completion of the first monolayer, reflecting the Bi-induced surface occupied states. A faint tail of states

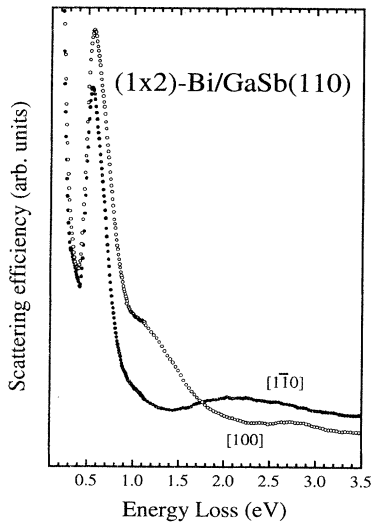

FIG. 6. Azimuthal dependence of the HREELS (scattering efficiency) data of the (1×2)-Bi/GaSb(110) interface at the two main azimuthal directions Φ=0° and Φ=90°. The azimuthal angle is defined as the angle between the incidence plane trace on the (110) surface and the [1-10] direction.

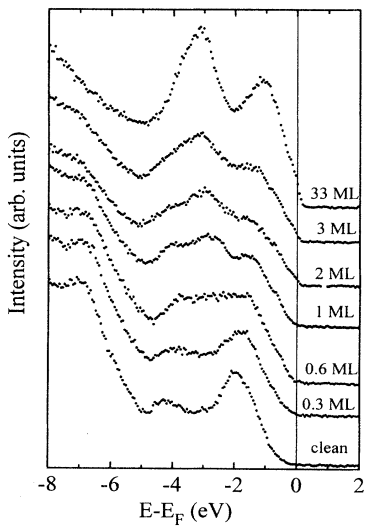

FIG. 7. Valence-band energy distribution curves (EDC's) of the Bi/GaSb(110) interface, as a function of Bi coverage. UPS data taken with He I discharge source (21.2-eV photon energy) and energy referred to the Fermi level. Spectra are stacked along the vertical axis for convenience.

crosses the Fermi level (E_F), indicating the presence of a low but unnegligible density of states at E_F. This detected onset of semimetallization confirms the previously discussed HREELS absorption data. Further deposition of Bi results in the establishment of a proper Fermi edge and of the typical Bi 6*p*-like bands, in agreement with other photoemission data.[48]

The EDC spectra of the (1×1)- and (1×2)-Bi phases are compared to the clean substrate and are shown in Fig. 8. The energy position of the main structures, as determined through a numerical second derivative of the data, is reported in Table II. The general slope of the valence band is in agreement with that recently obtained by angular-resolved photoemission by McIlroy *et al.* in a few points of the SBZ,[28] i.e., four main Bi-derived bands can be clearly identified. However, in our data we observe a light but important difference between the (1×1) and (1×2) phases, namely a small shift of the main peaks, and the growth of a shoulder just below the Fermi level for the (1×2) structure. This bump at 0.15-eV binding energy is related to momentum-integrated density of states (DOS), so that we cannot infer its very origin within the SBZ, but it denotes a distinct difference in the electronic valence-band structure between the stable (1×2)- and the (1×1)-Bi phases on GaSb(110).

A comparative analysis of the absorption excitations (by HREELS) and of the occupied states (by UPS) in the two different geometries of the Bi chemisorption on GaSb(110) leads to the following considerations: the highest occupied Bi-induced state presents a maximum in the integrated DOS at 0.15 eV in the (1×2) and at 0.65 eV in the (1×1) phase. The main absorption peak in HREELS is at 0.54 and 1.0 eV, respectively. This lets us infer the energy position for the lowest unoccupied Bi-derived level at ~0.4 eV above the Fermi energy for the stable (1×2)-Bi phase, while a slightly lower energy is expected (0.35 eV) in the (1×1)-Bi phase.

TABLE II. Energy positions (in eV) for the UPS photoemission structures in the (1×1) and (1×2) Bi phases at the Bi/GaSb(110) interface.

(1×1)-Bi		0.65	1.4	~2.8		4.1
(1×2)-Bi	0.15	0.75	1.5		~3.3	4.2

D. Electronic structure by EELS

The electron-energy-loss data relative to clean GaSb(110), (1×1)-Bi and (1×2)-Bi phases are shown in Fig. 9. The primary beam energy (E_p) is about 100 eV, ensuring surface sensitivity. The clean GaSb(110) spectrum shows the same features as first observed by van Laar, Huijser, and van Rooy[40] and also in agreement with more recent results:[32] valence-band to conduction-band transitions are localized at 3.2, 5.6, and 8.0 eV; the surface and bulk plasmon excitations at 9.9 and 14.7 eV; the surface Ga-3*d* exciton at 20 eV; the Ga-$M_{4,5}$ and Sb-$N_{4,5}$ absorption structures at ~23 and ~34 eV, respectively, due to the excitation of Ga-3*d* and Sb-4*d* electrons to the conduction band. The Ga surface exciton corresponds to the transition of electrons from the 3*d* core levels to the conduction band in the presence of the empty Ga dangling-bond states of the relaxed surface, which cause electron-hole pair interaction.[49] The exciton is, therefore, extremely sensitive to the surface quality and conditions, like the saturation or modification of the Ga dangling-bond states through absorption of atoms at the

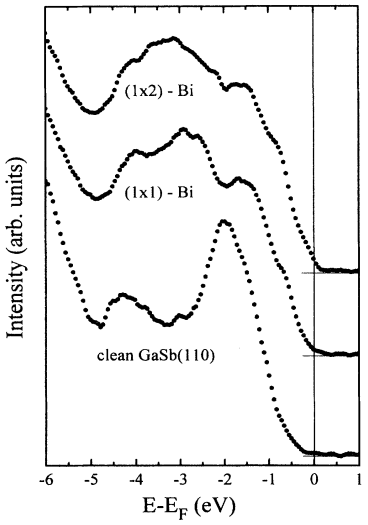

FIG. 8. UPS data in the valence-band region relative to the clean GaSb(110) surface, (1×1)-Bi monolayer as deposited, and stable (1×2)-Bi phase. Spectra are displaced along the vertical axis for convenience.

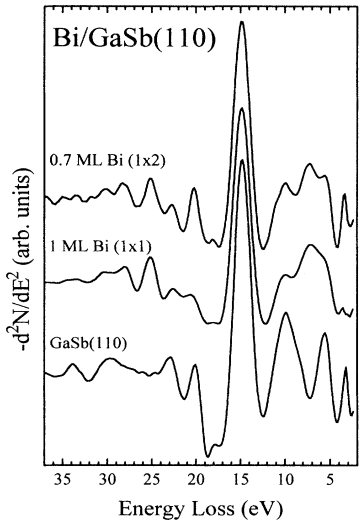

FIG. 9. EELS data relative to the clean GaSb(110) surface, the (1×1)-Bi monolayer as deposited, and the (1×2) stable Bi phase. Data have been taken in the first derivative mode; thereafter, they are numerically derived.

surface.[50]

The deposition of Bi causes a fast quenching of the surface exciton at the monolayer coverage, indicating the saturation of the Ga dangling bonds, and confirming the regular epitaxial growth of the first epitaxial Bi monolayer. The main absorption structures in the (1×1)-Bi monolayer are at 3.3, 5.6, and 7.7 eV, while they are at 3.3, 5.6, and 7.4 eV for the stable (1×2)-Bi phase. These features are due to interband electronic transitions between occupied and empty levels of the respective interfaces, reflecting the occurrence of Bi-induced electronic levels in the two phases. In particular, the 3.3- and 7.7-[7.4 for the (1×2)-Bi] eV structures are very likely derived from Bi-induced levels at the surface, as can be inferred from the shape evolution upon coverage in the original first-derivative data (not shown here for the sake of simplicity). On the other hand, the 5.6-eV peak cannot be straightly assigned to a transition between Bi-induced levels, but may involve substrate-related states.

The different energy of the electronic transitions involving Bi-related states for the (1×1)- and (1×2)-Bi phases denotes again the redistribution of the electronic occupied and empty Bi-induced levels, due to the structural reconstruction (although minor differences are present in the 3–10-eV energy range). Moreover, the Ga-surface exciton reappears in the EELS spectrum of the (1×2)-Bi phase, demonstrating the presence of free Ga dangling bonds at the surface. This evidence, along with the estimation of a Bi coverage of ~0.7 ML (Sec. III A),[29] suggests that the (1×2) reconstruction is characterized by a partial uncovering of the topmost Ga atoms, causing a charge redistribution between Bi and Ga, leaving a fraction of free Ga dangling-bond states. This situation might correspond to a Bi zigzag chain structure along the [1-10] azimuthal direction, in which a Bi atom close to a Ga atom is missing every chain over two, with a coupling between neighboring chains, thus producing a doubling of the unit cell in the [001] direction. Van Gemmeren and Johnson[36] propose a very similar structural model, where every second zigzag chain is removed, while McIlroy *et al.*[28] propose a similar surface reconstruction, characterized by a coupling of Bi neighboring chains at the coverage of 1 ML, which would also leave uncovered Ga atoms at the surface. However, whatever the actual position of the Bi atoms is, the (1×2) reconstruction [which is the stable phase for the Bi/GaSb(110) interface] corresponds to an atomic geometry with the Bi atoms preferentially bonded to Sb than to Ga, causing a charge redistribution between Bi, Sb, and Ga, and leaving free Ga dangling bonds at the surface.

E. Space-charge layer and semimetallization by HREELS

Further information about the dielectric nature of the Bi/GaSb(110) interface can be obtained from analysis of the vibrational and collective excitations at low energy, by means of HREELS. The dopant-induced free-carrier plasmon coupled with the optical active Fuchs-Kliewer phonon is influenced by the space-charge layer conditions in the subsurface region.[16,51,52] The HREELS data of the higher (*n*-type) doped sample in the low-energy region (0–130 meV) are collected in Fig. 10, as a function of the Bi coverage and for the (1×2)-Bi phase. The loss structure at 27.4 meV is due to the Fuchs-Kliewer phonon of GaSb, while the loss peak at 45 meV on the clean surface is due to the oscillations of the *n*-type dopant-induced free carriers. In order to get the normalized phonon peak intensity and plasmon-energy position as a function of coverage, a fit of the quasielastic peak, the phonon and the plasmon structures by Gaussian-Lorentzian curves was performed. The main influence of the Bi deposition is the plasmon-energy redshift (from 45.0 to 41.5 meV)—due to the depletion layer extension—and the phonon intensity attenuation—due to the adlayer screening effect—as shown in Fig. 11.

In order to gain more quantitative information on the space-charge layer formation and on the dielectric evolution of the interface, we use a semiclassical dielectric layer model.[53,54] In this model, each layer is described by its peculiar dielectric response,[54] and we reproduce the ex-

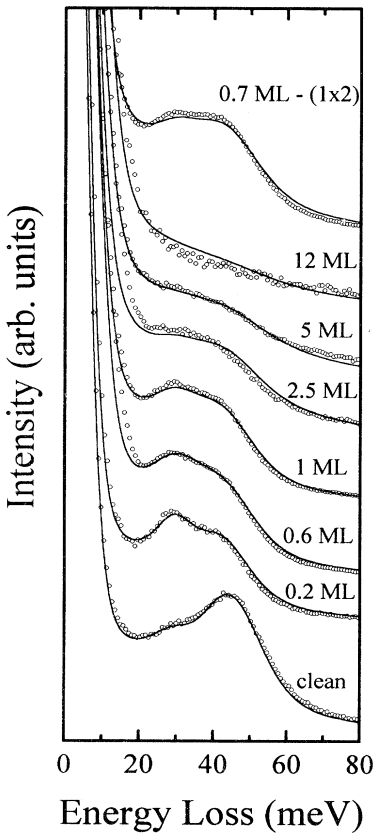

FIG. 10. HREELS data of the Bi/GaSb(110) interface, as a function of the Bi coverage, and for the (1×2)-Bi phase, in the energy region of the Fuchs-Kliewer optical phonon and of the dopant-induced free-carrier plasmon. *n*-type doped substrate, doping concentration $n \sim 2\times10^{18}$ cm^{-3}. Spectra are normalized to their respective elastic peak heights, and vertically stacked for the sake of clarity.

perimental data with an appropriate choice of the input parameters (energy, strength, and damping of the phonon and plasmon modes). More detail about this procedure can be found in Refs. 16 and 52. In particular, GaSb is described as a semi-infinite bulk region and a depletion layer. The bulk region has a dielectric function

$$\varepsilon(\omega)=\varepsilon_\infty+\frac{Q\omega_{\rm ph}^2}{\omega_{\rm ph}^2-\omega^2-i\gamma_{\rm ph}\omega}-\frac{\omega_{\rm pl}^2}{\omega^2+i\gamma_{\rm pl}\omega},$$

where $\omega_{\rm ph}$ and $\omega_{\rm pl}$ are the oscillator frequencies of the phonon and the dopant-induced free-carrier plasmon modes, respectively, and $\gamma_{\rm ph}$ and $\gamma_{\rm pl}$ are their respective energy-damping factors; ϵ_∞ is the infrared infinite frequency value (14.44) (Refs. 55 and 56) of the GaSb dielectric function, and Q is the phonon oscillator strength. The GaSb depletion layer is described by a dielectric function containing only ϵ_∞ and the phonon mode, being depleted of free carriers. The influence of the Bi layer at the lowest coverages can be quite well reproduced by the only variation of the depletion layer thickness, as the adlayer presents a semiconducting character. For coverages larger than 0.6 ML we can take into account the metallic screening effect of the Bi layer by introducing a Drude-like free-carrier plasmon in the adlayer.

The model spectra, calculated fitting the experimental data, are shown as continuous lines in Fig. 10. The parameters that were used and adjusted for fitting the experimental spectra are shown in Table III. Up to a coverage of ~0.6 ML we derive only an increases of the depletion layer thickness, with the main consequence of shifting the plasmon energy. Within the Schottky barrier approximation, we estimate a band-bending value $V_{\rm bb}\simeq(0.27\pm0.02)$ eV at 0.6-ML Bi on the n-type doped substrate, close to midgap. In the first adsorption stages, Bi induces filled electronic levels, described in the previous sections, which cause a depletion of free carriers from the GaSb subsurface region determining the measured barrier height. We would underline that in our measurements the electron current density impinging to the sample is extremely low, less than 1 nA/cm^{-2}, so that our estimation of the barrier height is not influenced by possible artifact like the surface photovoltaic effect.[57]

At higher Bi thickness, a good fit to the data can be obtained only taking into account a metallic character in the Bi topmost layer. This is particularly evident in the 1-ML (1×1)-Bi phase, for which the semimetallic dielectric response screens the underlying substrate-related mode (phonon).

For the stable (1×2)-Bi phase we estimate, with the same method, a $V_{\rm bb}$ of (0.14±0.02) meV. The lower barrier height, compared to the (1×1) phase, is due by a lower extension of the space-charge layer region in the underlying semiconducting substrate. This narrower depletion region can be induced by the Bi-related electronic density of states at the topmost layer, which correspond to a very ordered (1×2) structural configuration.

As for the (1×1), also the (1×2)-Bi phase presents a semimetallic screening. This result confirms the interface metallization we have observed in the energy-gap region as a continuum of intraband transitions (Sec. III B), and as a low density of states at the Fermi level (Sec. III C).

An important effect of the metallization on the Sb/GaAs(110) (Ref. 10) and Bi/GaAs(110) (Ref. 16) interfaces is the strong quenching of the substrate-related phonon and plasmon excitations. In the case of Bi/GaSb(110), we measure a definite attenuation of the phonon and plasmon intensities, but with a lower rate versus coverage than in the former interfaces. At a first sight this could be interpreted as a lower metallic screening, apparently contrasting that clear semimetallic behavior has been measured in the energy-gap region. We believe that such an apparent lower screening derives from the growth mode of Bi on GaSb(110): in fact, the first monolayer is semimetallic with a very low density of states at E_F, thus unable to really screen the underlying modes; moreover, the Bi clusters above the first epitaxial adlayer cover an average surface area of the order of 40% of the whole surface, at a coverage of ~4 ML (Sec. III A). Thus, Bi islands leave large areas (~60% of the total surface) constituted by 1 ML of adatoms uncovered by Bi clusters, so that the phonon mode can be probed unscreened through these areas, while it is almost fully screened by the Bi islands where they are formed. As a consequence, an average relatively high phonon and plasmon intensity is observed even at Bi thicknesses for which a clear semimetallization has been detected in the energy-gap region. In the (1×2)-Bi phase, the intensity

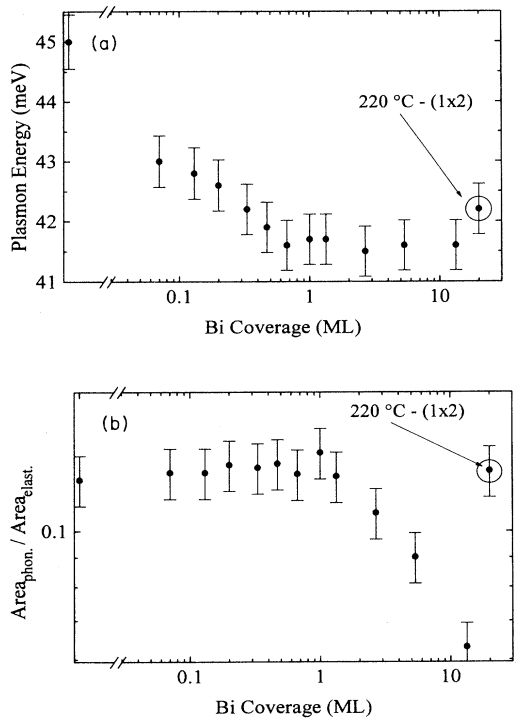

FIG. 11. Plasmon energy position and phonon intensity for the Bi/GaSb(110) interface, as a function of coverage and for the (1×2) annealed Bi phase (large dot). Data refer to the HREELS experiment shown in Fig. 10.

TABLE III. Parameters used for the dielectric model calculation fitting the experimental data. ε_∞ is the infrared infinite frequency value of the GaSb dielectric function; ω_{ph} and ω_{pl} are the phonon and the plasmon energies, respectively; γ_{ph} and γ_{pl} are the phonon and the plasmon dampings, respectively; Q is the phonon oscillator strength.

Layer	ε_∞	ω_{ph} (meV)	γ_p (meV)	Q	ω_{pl} (meV)	γ_{pl} (meV)
Bulk GaSb	14.45[a]	28.1[a]	0.2[a]	1.7[a]	205	20
Depletion layer	14.45[a]	28.1[a]	0.2[a]	1.7[a]		
Semimetallic Bi	100[b]				900–2000	500

[a]Data taken from Ref. 55.
[b]Data taken from Ref. 57.

of the substrate related modes is even higher than in the (1×1) stage, as a consequence of the large patches of bare substrate uncovered by Bi adatoms, corresponding to an equivalent thickness of 0.7 ML. These evidencies confirm our previous assumption of an "open" surface corresponding to the stable (1×2) structural model.

IV. SUMMARY AND CONCLUSIONS

We have presented an investigation of the growth mode and of the electronic properties of the Bi/GaSb(110) interface grown at RT and thermally stabilized. After the completion of the first epitaxial and ordered (1×1)-symmetry monolayer, Bi coalesces into islands covering ~40% of the surface area at a nominal thickness of ~11 Å. The (1×2)-symmetry stable phase, achieved by annealing at 220 °C corresponds to a Bi coverage of 0.7 ML. This coverage value and the presence of the Ga related surface exciton in the (1×2) phase may be explained by an "open" geometrical structure in which every but one row of Bi atoms is missing in the stable phase. This leads to a charge redistribution and is probably due to a preferential bonding of Bi to Sb than to Ga.

The valence-band structure of the (1×1)- and (1×2)-Bi phases have been characterized, determining the major Bi-induced occupied electronic levels. Both phases present huge absorption features at 1 and 0.54 eV, respectively, due to interband electronic transitions between Bi-related levels. At variance with other Bi/III-V(110) interfaces, both structural phases present a semimetallic nature, as detected by HREELS and photoemission. Finally, the Schottky barrier height has been estimated through analysis of the substrate-related phonon and dopant-induced free-carrier plasmon, leading to a value of 0.20 (0.14) eV in the (1×1) [(1×2)] phase.

ACKNOWLEDGMENTS

We are indebted to E. Angeli for his invaluable experimental assistance. Financial support from the Ministero per l'Università e per la Ricerca Scientifica e Tecnological (MURST) and from the Consiglio Nazionale delle Ricerche (CNR) is gratefully acknowledged.

[1]J. Carelli and A. Kahn, Surf. Sci. **116**, 380 (1982).
[2]C. B. Duke, A. Paton, W. K. Ford, A. Kahn, and J. Carelli, Phys. Rev. B **26**, 803 (1982).
[3]P. Skeath, C. Y. Su, W. A. Harrison, I. Lindau, and W. E. Spicer, Phys. Rev. B **27**, 6246 (1983).
[4]W. Pletschen, N. Esser, H. Münder, D. Zahn, R. Geurts, and W. Richter, Surf. Sci. **178**, 140 (1986).
[5]A. B. McLean and F. J. Himpsel, Phys. Rev. B **40**, 8425 (1989).
[6]J. J Joyce, J. Anderson, M. M. Nelson, and G. J. Lapeyre, Phys. Rev. B **40**, 10412 (1989).
[7]R. Ludeke, A. Taleb-Ibrahimi, R. M. Feenstra, and A. B. McLean, J. Vac. Sci. Technol. B **7**, 936 (1989); Phys. Rev. B **39**, 12925 (1989).
[8]Y. Hu, T. J. Wagener, M. B. Jost, and J. H. Weaver, Phys. Rev. B **40**, 1146 (1989).
[9]W. K. Ford, T. Guo, D. L. Lessor, and C. B. Duke, Phys. Rev. B **42**, 8952 (1990).
[10]G. Annovi, Maria Grazia Betti, U. del Pennino, and Carlo Mariani, Phys. Rev. B **41**, 11978 (1990).
[11]Maria Grazia Betti, M. Pedio, U. del Pennino, and Carlo Mariani, Phys. Rev. B **43**, 14317 (1991).
[12]Maria Grazia Betti, M. Pedio, U. del Pennino, and Carlo Mariani, Phys. Rev. B **45**, 14057 (1992).
[13]W. K. Ford, T. Guo, K. J. Wan, and C. B. Duke, Phys. Rev. B **45**, 11896 (1992).
[14]G. P. Srivastava, Phys. Rev. B **46**, 7300 (1992); **47**, 16616 (1993).
[15]G. P. Srivastava, J. Phys. Condens. Matter **5**, 4695 (1993).
[16]Valentina De Renzi, Roberto Biagi, Maria Grazia Betti, and Carlo Mariani, Phys. Rev. B **49**, 8198 (1994).
[17]Luca Gavioli, Maria Grazia Betti, Paolo Casarini, and Carlo Mariani, Phys. Rev. B **49**, 2911 (1994).
[18]A. Ruocco, N. Jedrecy, R. Pinchaux, M. Sauvage-Simkin, A. Waldhauer, Maria Grazia Betti, and Carlo Mariani, Phys. Rev. B **50**, 8004 (1994).
[19]Maria Grazia Betti, Carlo Mariani, N. Jedrecy, R. Pinchaux, A. Ruocco, and M. Sauvage-Simkin, Phys. Rev. B **50**, 14336 (1994).
[20]C. A. Swarts, W. A. Goddard, and T. C. McGill, J. Vac. Sci. Technol. **17**, 982 (1982).
[21]T. Kendelewicz, J. C. Woicik, A. Herrera-Gomez, K. E. Miyano, P. L. Cowan, B. A. Karlin, P. Pianetta, and W. E. Spicer, J. Vac. Sci. Technol. A **11**, 2351 (1993).
[22]F. Bechstedt, W. G. Schnmidt, and B. Wenzien, Europhys. Lett. **25**, 357 (1994).
[23]W. G. Schmidt, B. Wenzien, and F. Bechstedt, Phys. Rev. B

49, 4731 (1994).
[24]A. Tulke, A. Mattern-Klosson, and H. Lüth, Solid State Commun. **59**, 303 (1986); A. Tulke and H. Lüth, Surf. Sci. **178**, 131 (1986).
[25]P. Mårtensson, G. V. Hansson, M. Lähdeniemi, R. O. Magnusson, S. Wiklund, and J. M. Nicholls, Phys. Rev. B **33**, 7399 (1986).
[26]A. Herrera-Gomez, T. Kendelewicz, J. C. Woicik, K. E. Miyano, P. Pianetta, S. Southworth, P. L. Cowan, B. A. Karlin, and W. E. Spicer, J. Vac. Sci. Technol. A **11**, 2354 (1993).
[27]R. D. Meade and D. Vanderbilt, Phys. Rev. Lett. **63**, 1404 (1989).
[28]D. N. McIlroy, D. Heskett, A. B. McLean, R. Ludeke, H. Munekata, and N. J. DiNardo, J. Vac. Sci. Technol. B **11**, 1486 (1993); Phys. Rev. B **48**, 11 897 (1993).
[29]P. Casarini, thesis, Università di Modena, 1994.
[30]P. W. Chye, I. Lindau, P. Pianetta, C. M. Garner, C. Y. Su, and W. E. Spicer, Phys. Rev. B **18**, 5545 (1978).
[31]A. Walters and R. H. Williams, J. Vac. Sci. Technol. B **6**, 1421 (1988).
[32]D. Mao, A. Kahn, and L. Soonckindt, Phys. Rev. B **40**, 5579 (1989).
[33]K. M. Schirm, P. Soukiassian, P. S. Mangat, Z. Hurych, L. Soonckindt, and J. J. Bonnet, J. Vac. Sci. Technol. B **10**, 1867 (1992).
[34]T. Guo, R. E. Atkinson, and W. K. Ford, Phys. Rev. B **41**, 5138 (1990).
[35]C. Argile and G. E. Rhead, Surf. Sci. Rep. **10**, 277 (1989).
[36]T. van Gemmeren and R. L. Johnson, Surf. Sci. (to be published).
[37]Stefano Ossicini, Rossella Memeo, and Franco Ciccaci, J. Vac. Sci. Technol. A **3**, 387 (1985).
[38]M. G. Betti, C. Mariani, R. L. Johnson, and M. Sauvage-Simkin *et al.* (unpublished).
[39]S. M. Sze, *Physics of Semiconductor Devices* (Wiley, New York, 1981).
[40]J. van Laar, A. Huijser, and T. L. van Rooy, J. Vac. Sci. Technol. **14**, 894 (1977).
[41]V. L. Berkovits, L. F. Ivantsov, I. V. Makarenko, T. A. Minashvili, and V. I. Safarov, Solid State Commun. **64**, 767 (1987).
[42]L. H. Dubois, G. P. Schwartz, R. E. Camley, and D. L. Mills, Phys. Rev. B **27**, 3208 (1984).
[43]J. E. Demuth, B. N. J. Persson, and A. J. Schell-Sorokin, Phys. Rev. Lett. **51**, 2214 (1983).
[44]U. del Pennino, M. G. Betti, C. Mariani, C. M. Bertoni, S. Nannarone, I. Abbati, L. Braicovich, and A. Rizzi, Solid State Commun. **60**, 337 (1986).
[45]T.-C. Chiang and D. E. Eastman, Phys. Rev. B **22**, 2940 (1980).
[46]R. Manzke, H. P. Barnscheidt, C. Janowitz, and M. Skibowski, Phys. Rev. Lett. **58**, 610 (1987).
[47]X. D. Zhang, R. C. G. Leckey, J. D. Riley, J. Faul, and L. Ley, Phys. Rev. B **48**, 5300 (1993).
[48]H. J. Monkhorst and J. D. Pack, Phys. Rev. B **13**, 5188 (1976).
[49]G. J. Lapeyre and J. Anderson, Phys. Rev. Lett. **35**, 117 (1975).
[50]C. R. Bonapace, D. W. Tu, K. Li, and A. Kahn, J. Vac. Sci. Technol. B **3**, 1099 (1985).
[51]D. H. Ehlers and D. L. Mills, Phys. Rev. B **34**, 3939 (1986); **36**, 1051 (1987).
[52]R. Biagi, Carlo Mariani, and U. del Pennino, Phys. Rev. B **46**, 2467 (1992).
[53]D. L. Mills, Surf. Sci. **48**, 59 (1975); H. Ibach and D. L. Mills, *Electron Energy Loss Spectroscopy and Surface Vibrations* (Academic, New York, 1982).
[54]Ph. Lambin, J.-P. Vigneron, and A. A. Lucas, Phys. Rev. B **32**, 8203 (1984); Comput. Phys. Commun. **60**, 351 (1990).
[55]P. A. Thiry, J. L. Longueville, J. J. Pireaux, R. Caudano, H. Munekata, and M. Liehr, J. Vac. Sci. Technol. A **5**, 603 (1987); A. Mezerreg and C. Llinares, Phys. Status Solidi B **170**, 129 (1992).
[56]M. Alonso, R. Cimino, and K. Horn, Phys. Rev. Lett. **64**, 1947 (1990).
[57]S. Takano and H. Kawamura, J. Phys. Soc. Jpn. **28**, 348 (1970).